

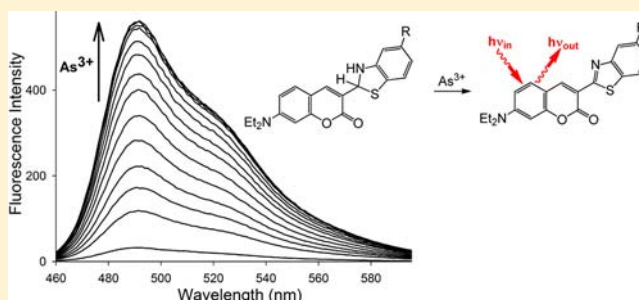
Synthesis and Properties of Arsenic(III)-Reactive Coumarin-Appended Benzothiazolines: A New Approach for Inorganic Arsenic Detection

Vivian C. Ezeh and Todd C. Harrop*

Department of Chemistry, The University of Georgia, 1001 Cedar Street, Athens, Georgia 30602, United States

Supporting Information

ABSTRACT: The EPA has established a maximum contaminant level (MCL) of 10 ppb for arsenic (As) in drinking water requiring sensitive and selective detection methodologies. To tackle this challenge, we have been active in constructing small molecules that react specifically with As^{3+} to furnish a new fluorescent species (termed a chemodosimeter). We report in this contribution, the synthesis and spectroscopy of two small-molecule fluorescent probes that we term ArsenoFluors (or AFs) as As-specific chemodosimeters. The AFs (AF1 and AF2) incorporate a coumarin fluorescent reporter coupled with an As-reactive benzothiazoline functional group. AFs react with As^{3+} to yield the highly fluorescent coumarin-6 dye (C6) resulting in a 20–25-fold fluorescence enhancement at $\lambda_{\text{em}} \sim 500$ nm with detection limits of 0.14–0.23 ppb in tetrahydrofuran (THF) at 298 K. The AFs also react with common environmental As^{3+} sources such as sodium arsenite in a THF/CHES (*N*-cyclohexyl-2-aminoethanesulfonic acid) (1:1, pH 9, 298 K) mixture resulting in a modest fluorescence turn-ON (1.5- to 3-fold) due to the quenched nature of coumarin-6 derivatives in high polarity solvents. Bulk analysis of the reaction of the AFs with As^{3+} revealed that the C6 derivatives and the Schiff-base disulfide of the AFs (SB1 and SB2) are the ultimate end-products of this chemistry with the formation of C6 being the principle photoproduct responsible for the As^{3+} -specific turn-ON. It appears that a likely species that is traversed in the reaction path is an As–hydride–ligand complex that is a putative intermediate in the proposed reaction path.



INTRODUCTION

Arsenic (As) and its compounds have received intense discussion of late in both the scientific community and general media. The controversial report of As^{5+} replacing P^{5+} in the DNA of certain bacteria initiated this interest; however, the definitive replacement of this toxic metalloid for phosphorus is still lacking and additional experiments by two independent groups suggest As is not incorporated into the DNA of these microbes.¹ There have also been reports of toxic levels of As in fruit juice (~20 ppb) and baby formula (~300 ppb) in early 2012.² These high levels were presumably a result of using contaminated water in the juice concentrates and organic brown rice syrup in the production of certain food products.² In fact, compounds of As are quite ubiquitous in the environment and originate primarily through mining, agricultural, and industrial activities.³ For example, crops like rice readily accumulate As compounds when planted in As-rich soils.⁴ Thus, exposure to toxic levels of As can readily occur through drinking contaminated water or eating foods produced from As contaminated soils.⁴ Exposure to As has been implicated in the rising incidence of a number of diseases; effects on the skin, liver, respiratory, and gastrointestinal tracts and cancers of the lung, bladder, and kidney have been reported.⁵ In a recent study, normal stem cells continuously exposed to 5 μM arsenite [$\text{As}^{3+}(\text{OH})_3$] in vitro acquired cancer stem cell phenotype by

18 weeks of exposure, potentially explaining how arsenite causes cancer.⁶ Additionally, As compounds are classified as group 1-nonthreshold carcinogens because there is no safe dose.⁷ To minimize the exposure of the population to arsenicals, the maximum contamination level (MCL) allowed in drinking water is set at 10 ppb (1 ppb = 1 $\mu\text{g}/\text{L}$) by the U.S. EPA and WHO (lowered from 50 ppb in 2001).⁸ There is currently no regulation for As levels in food. Regardless of the source, it is clear that As contamination and problems associated with it are vast and certainly not limited to third world countries.

The most common form of As in the environment is inorganic in nature (iAs) and includes compounds such as arsenite and arsenate ($[\text{As}^{5+}\text{O}_2(\text{OH})_2]^-$ or $[\text{As}^{5+}\text{O}_3(\text{OH})]^{2-}$) between pH 6 and 9.^{3g} The iAs can be further processed by soil microbes through methylation reactions to afford a variety of organic arsenicals such as methylarsonous acid [$\text{CH}_3\text{As}(\text{OH})_2$].⁹ When ingested by mammals, these As compounds (primarily As^{3+} compounds such as arsenite and methylarsonous acid) exhibit their toxicity by disrupting enzymes with active-site cysteine-thiol (Cys-SH) residues by forming strong As-SCys bonds and lead to misfolded proteins.¹⁰ Indeed, the

Received: August 6, 2012

Published: February 19, 2013



high affinity of As^{3+} for thiolates can alter the cellular redox homeostasis by forming a complex with glutathione (GSH) to generate the trigonal pyramidal $[\text{As}^{3+}(\text{SG})_3]$ complex. The reported formation constants for $[\text{As}(\text{SG})_3]$ are quite high although they are drastically different depending on the temperature and measurement technique ($\log \beta_3 = 32.0$, potentiometric at 298 K; $\log \beta_3 = 7.0$ at 310 K, colorimetric).¹¹

The relatively recent change in MCL coupled with the reports of high As levels in the US has led to new strategies to detect As in the environment. The development of such new strategies for As and the underlying chemistry that dictates the sensing phenomenon is thus of fundamental importance and is an overall goal of our research. Currently employed detection strategies for As utilize instruments such as ICP-MS and UV-vis spectroscopy in colorimetric methods. ICP-MS is the most employed method by the EPA as it is a reliable and sensitive detection strategy. However, ICP-MS is an expensive and bulky methodology that requires extensive sample preparation, thus making its use in the field challenging.¹² Colorimetric methods based on the Gutzeit reaction are field applicable, but this method suffers from false positives and produces highly toxic arsine gas (AsH_3) and mercury compounds as byproducts.^{12a} Thus, the development of other field-applicable, affordable, simple, and ppb-sensitive detection methods is in need. Fluorescence spectroscopy meets these requirements and has been widely utilized as a means of detecting numerous analytes.¹³ For example, bacterial biosensors have been developed for the detection of metalloids like arsenite, arsenate, and antimonite.¹⁴ The design involves engineering bacterial cells by linking genes that produce a fluorescence reporter protein such as luciferase or green fluorescent protein to the As resistance genes controlled by the *ars* operon. The non-pathogenic engineered microbes are then used to detect arsenite by measuring the bioluminescence produced.^{14,15} Recently, kits based on engineered *E. coli* strains were field-tested in Bangladesh, which demonstrated a detection limit of 4 ppb and a cost of \$1.50 per sample.¹⁶ It thus appears that fluorescence detection strategies for As are on the rise.

We published the synthesis and properties of As sensor molecules, called ArsenoFluors (AFs) in preliminary form, that report the presence of As^{3+} by fluorescence emission in organic media.¹⁷ These molecules rely on an As^{3+} -promoted redox conversion via transient coordination to the thiolate-S of a nonfluorescent benzothiazoline molecule into benzothiazole species that are structurally identical to the fluorescent coumarin-6 (C6) laser dye (Scheme 1). The objective of this contribution was to expand the AF library (AF1 and AF2), deduce probable mechanistic details of the As^{3+} turn-ON fluorescence of AFs, and test their capability to detect As^{3+} in aqueous conditions. We describe herein the synthesis and spectroscopic properties of AF1 and AF2 and their interactions

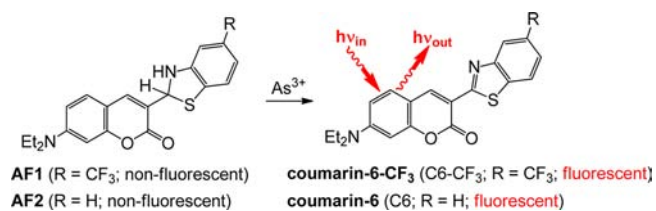
with As^{3+} . These molecules present an excellent platform for the selective and sensitive detection of As^{3+} (20–25-fold turn-ON; 0.1–0.2 ppb detection limits) in tetrahydrofuran (THF) at 298 K resulting in the formation of the fluorescent C6 derivatives. The end-products of this As-selective reaction appear to be due to transient coordination of As^{3+} to the N,S-chelate and rearrangement to an As^{3+} -hydride intermediate to liberate $\text{H}_2(\text{g})$, As^+ , and the Schiff-base disulfide compounds of the AFs through a reductive elimination reaction. We also demonstrate that the AF and As^{3+} reaction also afford C6 derivatives in aqueous mixtures and are potentially capable of reporting arsenite in a mixed $\text{H}_2\text{O}/\text{THF}$ medium.

EXPERIMENTAL SECTION

General Information. All reagents were purchased from commercial suppliers and used as received unless otherwise noted. Tetrahydrofuran (THF), diethyl ether (Et_2O), acetonitrile (MeCN), and dichloromethane (CH_2Cl_2) were purified by passage through activated alumina columns using an MBraun MB-SPS solvent purification system and stored over 4 Å molecular sieves under a dinitrogen (N_2) atmosphere before use. Triethylamine (Et_3N) was dried by storing over KOH and CaSO_4 in an N_2 atmosphere. Ethanol (EtOH) and methanol (MeOH) were dried by distilling from $\text{Mg}(\text{OEt})_2$ and $\text{Mg}(\text{OMe})_2$, respectively, under N_2 . A 50 mM CHES (*N*-cyclohexyl-2-aminoethanesulfonic acid) (pH = 9) solution was prepared by dissolving 1.0361 g of CHES in 100 mL of milli-Q water, and the pH was adjusted with either 1 M HCl or NaOH. Solvents were sufficiently degassed by at least three freeze-pump-thaw cycles before introduction into the glovebox. All solvents were filtered with a 0.45 μm nylon filter before spectroscopic measurements were recorded to remove particulates (primarily molecular sieves from anhydrous storage). All reactions were performed in an MBraun Unilab glovebox under an atmosphere of purified N_2 . Stock solutions of ArsenoFluor1 (AF1) and ArsenoFluor2 (AF2) were freshly prepared before all spectroscopic studies. 7-(Diethylamino)-2-oxo-2H-chromene-3-carbaldehyde,¹⁸ AF1,¹⁷ AF2,¹⁹ 6,6'-disulfanediyldis(3-trifluoromethyl)aniline,²⁰ and 2,2'-disulfanediyldianiline²¹ were synthesized according to literature procedures. The full characterization of 6,6'-disulfanediyldis(3-trifluoromethyl)aniline is presented in this work. All fluorescence sensing experiments in THF contain 5 mol-equiv of Et_3N unless stated otherwise.

Physical Methods. Electronic absorption spectra were obtained at 298 K using a Varian Cary-50 spectrophotometer containing a Quantum Northwest TC 125 temperature control unit. Fluorescence spectra were run at 298 K using a Varian Eclipse spectrofluorometer also containing the Quantum Northwest TC 125 temperature controller. All UV-vis and fluorescence samples were prepared in gastight Teflon-lined screw cap quartz cells with an optical pathlength of 1 cm. The quartz cells were cleaned thoroughly before each measurement by soaking in 10% HNO_3 for at least 3 h to remove trace metals and then rinsing with saturated NaHCO_3 solution, DI water, and MeOH. FTIR spectra were collected on a ThermoNicolet 6700 spectrophotometer running the OMNIC software. All samples were run as solids in a KBr matrix. ^1H and ^{13}C NMR spectra were recorded on either a Varian Unity Inova 500 MHz or Varian Mercury Plus 400 MHz NMR spectrometer at 298 K with chemical shifts referenced to tetramethylsilane ($\text{Si}(\text{CH}_3)_4$) or the residual protio signal of the deuterated solvent.²² ^{31}P NMR spectra were recorded on a Varian Unity Inova 500 MHz NMR spectrometer at 298 K with chemical shifts referenced to external 85% H_3PO_4 . Measurements of pH were performed on an Accumet pH meter from Fischer Scientific, model 25, with a combination electrode. A three point calibration with commercially available standards was performed before pH values were recorded. Low Resolution ESI-MS data were collected using a Perkin-Elmer Sciex API I Plus quadrupole mass spectrometer. Cyclic voltammetry (CV) measurements were performed with a PAR Model 273A potentiostat using a nonaqueous Ag/Ag^+ (0.01 M $\text{AgNO}_3/0.1$ M $^n\text{Bu}_4\text{NPF}_6$ in MeCN) reference electrode, Pt counter electrode, and a

Scheme 1. Sensing Strategy of the ArsenoFluors (AFs) and the Compounds Described in This Work



glassy-carbon (2 mm diameter) milli-working electrode under an Ar atmosphere. Measurements were performed at ambient temperature using 0.8–8.0 mM analyte in THF containing 0.1 M Bu_4NPF_6 as the supporting electrolyte. The “Maximize Stability” mode was utilized in the PAR PowerCV software utilizing a low-pass 5.3 Hz filter. Ferrocene (Fc) was used as an internal standard, and all potentials are reported relative to the Fc^+/Fc couple. Uncorrected melting points were obtained with a Laboratory Device MEL-TEMP II. All spectroscopic data were plotted by using the SigmaPlot 10.0 software package.

Synthesis of Compounds. *Caution!* Compounds containing arsenic (As) are toxic and should be handled with extreme care. Additionally, although no problems were observed in this work, perchlorate (ClO_4^-) salts of transition metals are potentially explosive and should also be handled with extreme care.

7-(Diethylamino)-3-(5-(trifluoromethyl)benzo[d]thiazol-2-yl)-2H-chromen-2-one (C6-CF₃). A solid mixture of 7-diethylaminocoumarin-3-aldehyde (0.0724 g, 0.2952 mmol), 4-(trifluoromethyl)-2-aminothiophenol hydrochloride (0.0679 g, 0.2952 mmol), and Et_3N (0.0851 g, 0.8409 mmol) was dissolved in 10 mL of EtOH to afford a light green solution. An orange colored precipitate formed in ~1 h after mixing, and the reaction was left to stir exposed to air for 48 h. The solvent was then removed via rotovap, and the ^1H NMR of the bulk orange residue revealed a mixture of AF1, C6-CF₃ (product of interest), and 7-diethylaminocoumarin-3-aldehyde. The desired C6-CF₃ compound was obtained from this mixture by recrystallization from hot EtOH to afford an orange solid (0.0303 g, 25%). m.p.: 242–243 °C. ^1H NMR (500 MHz, CDCl_3 , δ from $\text{Si}(\text{CH}_3)_4$): 1.27 (t, 6H, $\text{CH}_3\text{CH}_2\text{N}-$), 3.49 (q, 4H, $\text{CH}_3\text{CH}_2\text{N}-$), 6.58 (s, 1H), 6.69 (d, 1H), 7.51 (d, 1H), 7.59 (d, 1H), 8.04 (d, 1H), 8.27 (s, 1H), 8.93 (s, 1H). ^{13}C NMR (100.6 MHz, CDCl_3 , δ from $\text{Si}(\text{CH}_3)_4$): 12.64 (N- CH_2 - CH_3), 45.31 (N- CH_2 - CH_3), 97.20, 108.83, 110.31, 111.98, 119.42 (q, $J = 4.4$ Hz), 120.76 (q, $J = 3.0$ Hz), 122.34, 127.29 (q, $J = 273.8$ Hz, CF_3), 128.82 (q, $J = 32.4$ Hz), 131.21, 139.79, 142.83, 152.37, 152.62, 157.45, 161.19 (C=N), 164.13 (C=O) unless noted ^{13}C peaks are singlets, splitting is due to coupling of the ^{13}C and ^{19}F nuclei. FTIR (KBr pellet), ν_{max} (cm^{-1}): 3083 (w), 2977 (w), 2931 (w), 2896 (w), 2872 (w), 1705 (s, C=O), 1697 (s, C=O), 1620 (vs, C=N), 1584 (vs), 1515 (vs), 1478 (w), 1419 (m), 1378 (w), 1352 (m), 1328 (vs), 1292 (w), 1277 (w), 1264 (w), 1228 (m), 1196 (s), 1150 (w), 1132 (s), 1112 (m), 1094 (w), 1070 (w), 1050 (w), 1015 (w), 977 (w), 950 (m), 884 (w), 821 (m), 811 (w), 799 (w), 770 (m), 708 (w), 679 (w), 669 (w), 636 (w), 530 (w), 512 (w), 472 (w), 442 (w). UV-vis (THF, 298 K) λ_{max} nm (ϵ , $\text{M}^{-1} \text{cm}^{-1}$): 464 (52 900); UV-vis (THF/CHES (1:1, pH 9), 298 K) λ_{max} nm (ϵ , $\text{M}^{-1} \text{cm}^{-1}$): 473 (52,000). LRMS-ESI (m/z): $[\text{M} + \text{H}]^+$ calcd for $\text{C}_{21}\text{H}_{18}\text{F}_3\text{N}_2\text{O}_2\text{S}$, 419.1; found, 419.2.

6,6'-Disulfanediybis(3-trifluoromethyl)aniline. To a 3 mL Et_2O solution of 4-(trifluoromethyl)-2-aminothiophenol hydrochloride (1.0907 g, 4.7494 mmol) was added Et_3N (0.5012 g, 4.9531 mmol) affording a light yellow heterogeneous mixture. The mixture was sonicated for 10 min and filtered revealing a yellow filtrate containing the 4-(trifluoromethyl)-2-aminothiophenol and an off-white solid ($\text{Et}_3\text{N}\cdot\text{HCl}$ based on IR). After removal of the Et_2O , the yellow oil was dissolved in 30 mL of MeCN, and to this solution was added NaI (0.1450 g, 0.9674 mmol) and FeCl_3 (0.0758 g, 0.4732 mmol) resulting in a dark green mixture which was stirred at RT for 10 min. The MeCN was removed via rotovap to afford a dark brown oil; then, 30 mL of a 1% sodium thiosulfate ($\text{Na}_2\text{S}_2\text{O}_3$) solution was added to provide a yellow precipitate. A 50 mL portion of CH_2Cl_2 was added to extract the yellow precipitate, and the resulting yellow solution was dried with Na_2SO_4 , filtered, and concentrated to afford the off-white solid product (0.3754 g, 0.9767 mmol, 41%). ^1H NMR (500 MHz, CDCl_3 , δ from $\text{Si}(\text{CH}_3)_4$): 4.54 (s, 2H, NH_2), 6.81 (d, 1H), 6.94 (s, 1H), 7.23 (d, 1H). ^{13}C NMR (100.6 MHz, CDCl_3 , δ from $\text{Si}(\text{CH}_3)_4$): 111.80 (q, $J = 4.0$ Hz), 114.49 (q, $J = 4.0$ Hz), 121.80 (s), 123.83 (q, $J = 272.7$ Hz, CF_3), 133.68 (q, $J = 32.2$ Hz), 136.88 (s), 148.63 (s); unless noted ^{13}C peaks are singlets, splitting is due to coupling of the ^{13}C and ^{19}F nuclei. FTIR (KBr), ν_{max} (cm^{-1}): 3408 (m), 2963 (m), 1620 (s), 1488 (m), 1437 (s), 1339 (vs), 1282 (m), 1262 (s), 1167

(s), 1120 (vs), 1081 (vs), 1023 (s), 920 (m), 867 (m), 804 (s), 690 (m). LRMS-ESI (m/z): $[\text{M} + \text{H}]^+$ calcd for $\text{C}_{14}\text{H}_{11}\text{F}_6\text{N}_2\text{S}_2$, 385.0; found, 385.0.

3,3'-((1E,1'E)-((Disulfanediybis(3-(trifluoromethyl)-6,1-phenylene)bis(azanylylidene)bis(methanylylidene)bis(7-(diethylamino)-2H-chromen-2-one) (SB1). A solid batch of 7-diethylaminocoumarin-3-aldehyde (0.3924 g, 1.600 mmol) and 6,6'-disulfanediybis(3-trifluoromethyl)aniline (0.3072 g, 0.7993 mmol) was dissolved in a mixture of propionitrile (6 mL), EtOH (3 mL), CHCl_3 (3 mL), and CH_2Cl_2 (5 mL) to give an orange colored slurry. The mixture was then refluxed for 7 h and stirred at RT for 12 h in the presence of 3 Å molecular sieves resulting in a bright orange colored mixture. A 20 mL portion of CH_2Cl_2 was added to the flask, and the reaction was filtered to remove mol-sieves. The filtrate was then concentrated via rotovap to afford an orange solid, which was washed with 20 mL of Et_2O to remove unreacted aldehyde and dried to afford 0.1520 g (0.1812 mmol, 23%) of orange solid product. m.p.: 202–204 °C. ^1H NMR (400 MHz, CDCl_3 , δ from $\text{Si}(\text{CH}_3)_4$): 1.25 (t, 6H, $\text{CH}_3\text{CH}_2\text{N}-$), 3.48 (q, 4H, $\text{CH}_3\text{CH}_2\text{N}-$), 6.53 (s, 1H), 6.65 (d, 1H), 7.37 (m, 2H), 7.48 (d, 1H), 7.64 (d, 1H), 8.64 (s, 1H), 8.81 (s, 1H). ^{13}C NMR (100.6 MHz, CDCl_3 , δ from $\text{Si}(\text{CH}_3)_4$): 12.67 (N- CH_2 - CH_3), 45.32 (N- CH_2 - CH_3), 97.45, 109.10, 110.11, 114.46 (q, 4.0 Hz), 114.63, 123.38 (q, 3.6 Hz), 124.09 (q, 272.0 Hz), 125.64, 129.68 (q, 33.2 Hz), 131.66, 136.39, 142.71, 149.09, 152.73, 156.15, 158.22 (C=N), 162.32 (C=O); unless noted ^{13}C peaks are singlets, splitting is due to coupling of the ^{13}C and ^{19}F nuclei. FTIR (KBr pellet), ν_{max} (cm^{-1}): 3082 (w), 2976 (m), 2930 (w), 2903 (w), 2871 (w), 1706 (s, C=O), 1621 (vs, C=N), 1582 (vs), 1519 (vs), 1484 (m), 1420 (m), 1378 (w), 1359 (s), 1331 (vs), 1276 (m), 1257 (m), 1229 (m), 1188 (s), 1111 (vs), 1072 (m), 1051 (m), 950 (w), 938 (w), 886 (w), 821 (m), 810 (m), 769 (w), 705 (w), 667 (w), 638 (w), 472 (w). LRMS-ESI (m/z): $[\text{M} + \text{H}]^+$ calcd for $\text{C}_{42}\text{H}_{37}\text{F}_6\text{N}_4\text{O}_4\text{S}_2$, 839.2; found, 839.2. UV-vis (THF, 298 K) λ_{max} nm (ϵ , $\text{M}^{-1} \text{cm}^{-1}$): 469 (85 000); UV-vis (THF/CHES (1:1, pH 9), 298 K) λ_{max} nm (ϵ , $\text{M}^{-1} \text{cm}^{-1}$): 482 (68 000).

3,3'-((1E,1'E)-(2,2'-Disulfanediybis(2,1-phenylene)bis(azan-1-yl-1-ylidene)bis(methan-1-yl-1-ylidene)bis(7-(diethylamino)2H-chromen-2-one) (SB2). A solid batch of 2-aminothiophenol disulfide (0.0274 g, 0.110 mmol) and 7-diethylaminocoumarin-3-aldehyde (0.0569 g, 0.232 mmol) was dissolved in 12 mL of MeOH/ CH_2Cl_2 (1:1) to afford a yellow colored solution. The reaction was then taken to reflux for 16 h resulting in no visible color change. Upon cooling to RT, the solvent was removed via rotovap to afford an orange residue, which was then washed with 10 mL of Et_2O and dried to afford a yellow solid product (0.0145 g, 0.0206 mmol, 19%). m.p.: 210 °C dec ^1H NMR (400 MHz, CDCl_3 , δ from $\text{Si}(\text{CH}_3)_4$): 1.25 (t, 7H, $\text{CH}_3\text{CH}_2\text{N}-$, integrates slightly high due to overlap with trace Et_2O from workup), 3.48 (q, 5H, $\text{CH}_3\text{CH}_2\text{N}-$, integrates slightly high due to overlap with trace Et_2O from workup), 6.52 (s, 1H), 6.64 (d, 1H), 7.16 (m, 3H), 7.47 (d, 1H), 7.61 (d, 1H), 8.64 (s, 1H), 8.77 (s, 1H). ^{13}C NMR (100.6 MHz, CDCl_3 , δ from $\text{Si}(\text{CH}_3)_4$): 12.67 (N- CH_2 - CH_3), 45.23 (N- CH_2 - CH_3), 97.38, 109.16, 109.90, 115.29, 117.57, 125.88, 127.12, 131.42, 132.43, 142.11, 148.96, 152.30, 154.40, 157.94 (C=N), 162.47 (C=O). FTIR (KBr pellet), ν_{max} (cm^{-1}): 3052 (w), 2970 (w), 2925 (w), 2868 (w), 1717 (s, C=O), 1618 (vs, C=N), 1583 (vs), 1560 (s), 1514 (vs), 1455 (m), 1418 (m), 1379 (m), 1354 (m), 1300 (w), 1258 (s), 1188 (s), 1169 (m), 1133 (s), 1076 (m), 912 (w), 820 (w), 795 (w), 741 (w), 685 (w), 654 (w), 601 (w), 468 (w). LRMS-ESI (m/z): $[\text{M} + \text{H}]^+$ calcd for $\text{C}_{40}\text{H}_{39}\text{N}_4\text{O}_4\text{S}_2$, 703.2; found, 703.2. UV-vis (THF, 298 K) λ_{max} nm (ϵ , $\text{M}^{-1} \text{cm}^{-1}$): 460 (65 000).

Bulk Reactions. The bulk reaction of AF1 with As^{3+} was reported in a previous account.¹⁷

AF2 Reaction with As^{3+} . A solid batch of AF2 (0.0943 g, 0.2676 mmol) was dissolved in 6 mL of THF containing 0.0271 g (0.2678 mmol) of Et_3N resulting in a light green homogeneous solution. To this mixture was then added a 6 mL THF solution of AsI_3 (0.0615 g, 0.1350 mmol), and the color changed instantaneously to red–orange with the formation of a pale precipitate ($\text{Et}_3\text{N}\cdot\text{HI}$). After stirring at RT in the glovebox for 2 h, the off-white precipitate was filtered off affording a red filtrate. This filtrate was concentrated to yield a red

solid (0.1950 g, slightly greater than 100% recovery presumably due to workup conditions), and the ^1H NMR was taken, which revealed a mixture of AF2, C6, and the Schiff-base disulfide SB2.

AF2 Reaction of As^{3+} with Diphenylphosphinoethane (dppe). A solid batch of AF2 (0.0279 g, 0.0792 mmol) was dissolved in 3 mL of THF containing Et_3N (0.0400 g, 0.3953 mmol) to afford a light green solution. To this solution was then added a 3 mL THF solution of AsI_3 (0.0360 g, 0.0790 mmol) that instantaneously generated a dark red heterogeneous mixture. After 30 min stirring at RT, a clear and colorless 3 mL THF solution of dppe (0.0315 g, 0.0791 mmol) was added, which resulted in no visible color change. The reaction was left to stir for 1 h at RT before the solvent was removed in vacuo to afford a red oily solid. A 5 mL solution of Et_2O was added to the solid to remove any unreacted dppe, and the solution was left to stir for 30 min. This mixture was then filtered to remove the insoluble dark red solid (0.0840 g), and the resulting red filtrate was concentrated to dryness to afford an orange colored solid (0.0485 g).

Red Solid Characterization. LRMS-ESI (m/z) {positive mode}: 353.0 ($\text{AF2} + \text{H}^+$); 473.0 ($[\text{As}(\text{dppe})]^+$); 703.2 ($\text{SB2} + \text{H}^+$); {negative mode} 126.8 (I^-). ^{31}P NMR (202 MHz, CD_2Cl_2 , δ from H_3PO_4): major peak, 61.63 (s) ($[\text{As}(\text{dppe})]^+$); minor peaks, 51.00 (d) (appear within 30 min of sample preparation when precipitate starts forming in the NMR tube) and 31.91 (t) (assigned as phosphine oxide).²³

Orange Solid Characterization. 31.44 (t) (phosphine oxide), 27.60 (d) (not assigned), -12.17 (t) (unreacted dppe). NB: The compound formed is stable only for a short time in CD_2Cl_2 at RT, after a few min an unknown insoluble orange-colored decomposition product is formed and a doublet at ~ 50 ppm in the ^{31}P NMR appears. The appearance of these peaks are also observed in the original preparation of $[\text{As}(\text{dppe})]^+$.²³

Spectroscopic Measurements. UV-Vis and Fluorescence. Absorption and fluorescence samples were prepared in anhydrous THF in an N_2 -filled glovebox at ambient temperatures for studies in organic media. Milli-Q grade water (18.2 $\text{M}\Omega\cdot\text{cm}$) was used to prepare samples for aqueous media studies. Stock solutions of AF1, AF2, and AsI_3 were prepared fresh in degassed THF on the day of the experiment while stock solutions of NaAsO_2 were prepared in degassed Milli-Q water. The blank solution for the aqueous studies consists of THF/CHES (1:1, pH 9). The excitation wavelengths (λ_{ex}) were set at 460 nm (AF1 in THF at 298 K), 471 nm (AF1 in THF/CHES (1:1) at 298 K), and 443 nm (AF2 in THF at 298 K) unless otherwise stated. The fluorescence readings were recorded 30 min after addition of As^{3+} to allow for complete reaction. All measurements were performed in triplicate, and we report the average.

Competition Studies. AsI_3 was used to prepare the As^{3+} stock solutions in THF. THF solutions of Na^+ , Ca^{2+} , Mg^{2+} , Mn^{2+} , Ni^{2+} , Cu^{2+} , Zn^{2+} , Pb^{2+} , and Cd^{2+} were prepared from their perchlorate salts; solutions of Fe^{3+} and Hg^{2+} were prepared from their chloride salts, and a solution of Co^{2+} was prepared from $[\text{Co}(\text{H}_2\text{O})_6](\text{BF}_4)_2$. A typical measurement contained 0.45 μM AF1 or AF2 containing 5 mol-equiv of base (Et_3N , 2.25 μM), while 10 mol-equiv of metal ions or metalloids were used. The $[\text{As}^{3+}]$ in each competition study was 4.5 μM . As above, fluorescence readings were obtained 30 min after the addition of the metal aliquot.

Quantum Yield (Φ_f). Coumarin 1 ($\Phi_f = 0.70$ in EtOH)²⁴ was used as a standard in the calculation of the quantum yield of AF1 and AF2 and its As^{3+} reaction product, namely, coumarin-6 (C6). Quantum yield studies with AF1 have been reported previously.¹⁷ In this study, solutions of the samples and standards with absorbance values in the range of 0.010–0.018 at $\lambda_{\text{ex}} = 379$ nm were prepared. The corrected emission spectra were obtained at 298 K with an excitation and emission slit width of 5 nm and integrated by measuring the area under the corrected emission spectrum from 389 to 600 nm. The quantum yield was calculated by the comparative method with the following equation:

$$\text{QY}_x = \text{QY}_s \cdot [A_x/A_s] \cdot [F_s/F_x] \cdot [n_x/n_s]^2$$

where QY: quantum yield; A: integrated area under the corrected fluorescence spectrum; F: fraction of light absorbed ($1 - 10^{-D}$); D:

absorbance (optical density); n = refractive indices of the solvent (EtOH = 1.3614; THF = 1.4072); subscript x: sample; subscript s: standard

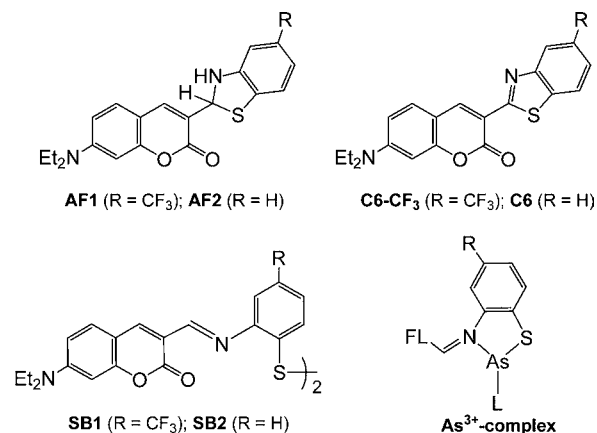
Fluorescence readings were obtained 30 min after the addition of the As^{3+} aliquot. All measurements were performed at least in triplicate, and we report the average.

Detection Limit. Detection limits were calculated on the basis of the signal-to-background (S/B) ratio method that describes a $S/B \geq 3$ as the detection limit.²⁵ The concentration of AF1 and AF2 used to determine the detection limit value was the same as in the fluorescence measurements (0.45 μM). Various stock solutions (0.79 μM and 0.18 μM) of AsI_3 were prepared by serial dilution, and the S/B ratio was obtained by comparing the fluorescence intensity of As^{3+} -containing solutions from 0.061 to 17 nM to the fluorescence intensity of the AFs without As^{3+} .

RESULTS

As we reported in a preliminary account,¹⁷ AF1 reacts with As^{3+} salts to afford the fluorescent benzothiazole C6-CF₃ (see Scheme 1, Chart 1). This product was clearly formed in the

Chart 1. Structures of the As^{3+} sensors (AF1 and AF2) and other products in the As^{3+} and AF reaction.^a



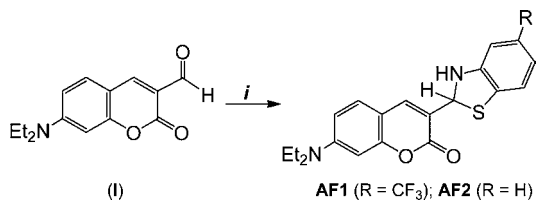
^aFor the As^{3+} complex, L = solvent or other anionic ligand present in the reaction mixture such as a halide; FL = remainder of the coumarin fluorophore.

reaction, which was verified by a variety of spectroscopic techniques such as UV-vis and NMR. A primary goal of this contribution was to deduce the mechanistic details of the As^{3+} turn-ON fluorescence. As such, several other products (other than C6) were proposed in this reaction and are displayed in Chart 1. These include the Schiff-base disulfide derivatives of AF1 and AF2 (denoted as SB1 and SB2, respectively) and the corresponding As^{3+} ligated compounds. Additionally, another AF (denoted as AF2) was synthesized and characterized as a sensor for comparison purposes. As^{3+} reactions with AF2 form the exact commercially available laser dye known as coumarin-6 (C6) (Scheme 1, Chart 1).

Syntheses of Compounds. The AFs comprise a benzothiazoline group that is sensitive to the presence of metal ions. Given the thiophilicity¹¹ of As^{3+} and the results of previous work in our lab,²⁶ we anticipated the AF compounds to react with As^{3+} to yield the fluorescent benzothiazoles (C6 compounds) in addition to other products (Scheme 1, Chart 1). The syntheses of AF1 and AF2 have been reported previously and involve the condensation of 7-(diethylamino)-coumarin-3-aldehyde (I) and the appropriate 2-aminothiophenol in EtOH at RT to afford AF1 (88%) and AF2 (75%) as

yellow solids in high yields, which is illustrated in Scheme 2.^{17,19} The C6 compounds (oxidized benzothiazole form of the

Scheme 2. Synthesis of AFs^a



^a(i) 4-(Trifluoromethyl)-2-aminothiophenol-HCl (for AF1) or 2-aminothiophenol (for AF2), EtOH, Et₃N, 298 K, 6–8 h.

AFs) were independently synthesized (or purchased in the case of coumarin-6) in order to have a spectroscopic signature to compare with the As³⁺–AF reaction products. For example, the benzothiazole compound C6-CF₃ was synthesized by air oxidation of AF1 to result in the coumarin as an orange solid in moderate yield (25%) after recrystallization from hot EtOH. The in situ synthesis and characterization of C6-CF₃ through the reaction of AF1 and As³⁺ in THF was previously reported by our laboratory and match the spectroscopic signatures obtained for the independent synthesis of C6-CF₃.¹⁷ Additionally, AF1 and AF2 in the solid state are stable for weeks when stored under anaerobic conditions and in the dark as judged by ¹H NMR and UV–vis spectroscopies. However, organic solutions (THF, CH₂Cl₂) of AF2 spontaneously oxidized to C6 under normal laboratory (aerobic) environments whereas solutions of AF1 were stable to oxygen over several days.

Since benzothiazoline groups are known to exist in resonance with their corresponding Schiff-base or imine-thiol form in solution,²⁷ we monitored the ¹H NMR spectra of AF1 and AF2 over time (t = 24 h). The resulting RT ¹H NMR spectra of AF1 or AF2 in CDCl₃ display only one set of peaks indicating that these compounds exist in the benzothiazoline form in both the solid (based on X-ray crystallography of AF1¹⁷ and FTIR spectra) and solution state. The exclusivity of this form is further evident in the D₂O-exchangeable proton resonance of the NH arising from the benzothiazoline form (4.89 ppm for AF1; 4.71 ppm for AF2 in CDCl₃) and absence of the downfield-shifted azomethine (R–CH=NR') proton resonance that would be expected for the Schiff-base at ~9 ppm.

As the Schiff-base disulfide analogues of AF1 and AF2 (SB1 and SB2, respectively; see Chart 1) are potential products in the AF and As³⁺ reactions, these compounds were also synthesized and characterized. Thus, SB1 and SB2 were constructed by Schiff-base condensation reactions between aldehyde I and the appropriate aromatic amine disulfide in low yields (19–23%, see Scheme S1 in the Supporting Information). The purity of the orange solid SB compounds was verified by several spectroscopic techniques, which included ¹H/¹³C NMR, FTIR, ESI-MS, UV–vis, and fluorescence spectroscopies (vide infra). The SBs are not as stable as the AFs, and slow (weeks) hydrolysis occurred resulting in reformation of aldehyde I and the amine even in the solid state.

Photophysical Properties. The photophysical properties of the As-sensors AF1 and AF2, along with probable reaction products, are presented for selected compounds in Figures 1–3 and S1–S3 (Supporting Information). The electronic absorption spectra of the AF, C6, and SB compounds all display

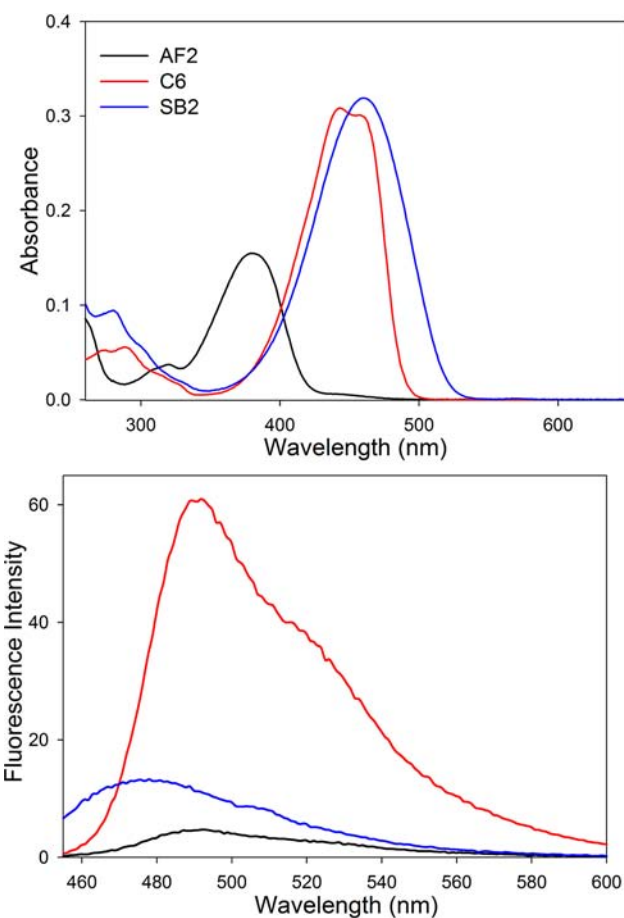


Figure 1. (Top) UV–vis spectra of AF2 (black trace, 5.7 μ M), C6 (red trace, 5.7 μ M), and SB2 (blue trace, 4.9 μ M). (Bottom) Fluorescence spectra of AF2 (black trace, 0.57 μ M), C6 (red trace, 0.53 μ M), and SB2 (blue trace, 0.59 μ M). $\lambda_{\text{ex}} = 443$ nm; slit width = 5 nm. All spectra recorded in THF at 298 K.

somewhat distinct UV–vis absorption profiles, which allowed for straightforward identification of these species (Figures 1 and S1, Supporting Information). AF1 and AF2 display broad intense maxima at 385 nm (ϵ : 29 000 M⁻¹ cm⁻¹)¹⁷ and 379 nm (ϵ : 26 300 M⁻¹ cm⁻¹), respectively, in THF at 298 K (Figures 1 and S1, Supporting Information) and is assigned as an n – π^* charge-transfer transition from the Et₂N-group to the π cloud of the coumarin ring.^{18b,28} These maxima red-shift in aqueous/organic mixtures; λ_{max} : 393 nm (ϵ : 29 500 M⁻¹ cm⁻¹) for AF1 in THF/CHES (1:1, pH 9, 298 K) (Figure S2, Supporting Information). For the C6 analogues, the UV–vis displayed several λ_{max} in the UV region, but the most distinctive absorption feature was the broad double-humped band centered at ~450–455 nm (Figures 1 and S1, Supporting Information). These bands are nearly twice the intensity ($\epsilon \sim 55$ 000 M⁻¹ cm⁻¹) of those associated with the AFs ($\epsilon \sim 30$ 000 M⁻¹ cm⁻¹). The UV–vis spectra of the SB compounds are somewhat similar to C6 but with lower energy and more intense maxima (λ_{max} : 469 nm, ϵ : 85 000 M⁻¹ cm⁻¹ for SB1; λ_{max} : 460 nm, ϵ : 65 000 M⁻¹ cm⁻¹ for SB2). Extensive delocalization over two coupled π -systems through the disulfide bond or π – π stacking of the aromatic molecules presumably lead to such an effect. Analogous to AF1, the absorption spectra of C6-CF₃ and SB1 shift to lower energy in a THF/pH 9 CHES mixture (Figure S2, Supporting Information).

The fluorescence profiles of the AFs and their potential As^{3+} reaction products are even more distinct than their corresponding UV-vis spectra. The fluorescence properties of AF1 and C6- CF_3 have already been reported.¹⁷ In sum, AF1 exhibits minimal fluorescence (fluorescence quantum yield = $\Phi_f = 0.004$; $\lambda_{\text{ex}} = 385$ nm), which is in stark contrast to the oxidized analogue C6- CF_3 ($\lambda_{\text{em}} = 496$ nm). For comparative purposes, SB1 was included in this study and also demonstrated low fluorescence intensity (Figure S1, bottom, Supporting Information). Much like AF1 and its oxidized counterparts, the AF2-derived compounds also demonstrate similar fluorescence properties. AF2 ($\Phi_f = 0.007$; $\lambda_{\text{ex}} = 379$ nm) and SB2 are essentially nonemissive whereas C6 is highly emissive ($\lambda_{\text{em}} = 492$ nm) (Figure 1, bottom). Taken together, the As^{3+} -induced oxidation of the AFs to C6 derivatives represent a suitable reaction path to exploit for fluorescence sensing of As^{3+} cations.

As^{3+} Response of AFs. The addition of As^{3+} salts such as AsI_3 or AsCl_3 to THF solutions of the AFs resulted in instantaneous UV-vis and fluorescence changes of the reaction mixture, which are indicative of C6 formation. For example, mixing 0.5 mol-equiv of As^{3+} with AF2 in THF resulted in a decrease in the 379 nm peak and the appearance of two new peaks at 290 and 443 nm over the course of 30 min at 298 K (Figure 2). An isosbestic point at 400 nm is observed in the

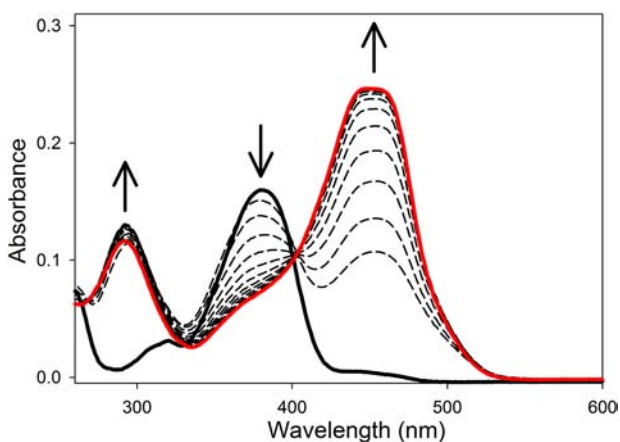


Figure 2. UV-vis spectral monitor of AF2 (6.4 μM) with 0.5 mol-equiv As^{3+} in THF at 298 K. Each trace recorded at 5 min intervals, total time = 1 h. Initial trace (bold black) and final trace (bold red). Arrows depict direction of change.

UV-vis spectral monitor indicating a clean transformation. The final UV-vis spectrum exhibits a broad and nearly double-humped peak that is similar to commercially obtained C6 in THF to support C6 formation when AF2 and As^{3+} react (Figure 2). The end result is the same regardless of the ratio employed. For example, a 1:1 As^{3+} /AF mixture afforded a similar spectral profile. This result suggests that the reaction path is the same with different stoichiometries. A similar UV-vis change also resulted for AF1 under identical reaction conditions suggesting that C6 compounds are a general product when AFs react with As^{3+} .¹⁷

The established formation of C6 derivatives from UV-vis was also verified by fluorescence spectroscopy. For example, addition of As^{3+} to nonfluorescent AF2 resulted in a 20-fold increase in fluorescence intensity ($\Phi_f(\text{As}) = 0.121$) with an emission spectrum matching C6 ($\lambda_{\text{em}} = 492$ nm) and giving rise to the OFF-ON fluorescent response to As^{3+} (Figure 3, top). This fluorescence response is comparable to the 25-fold

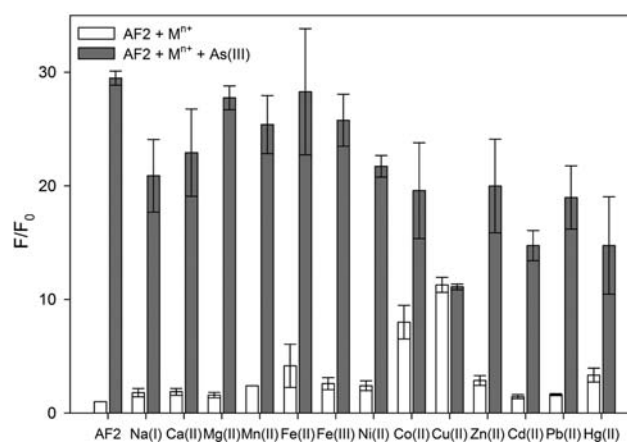
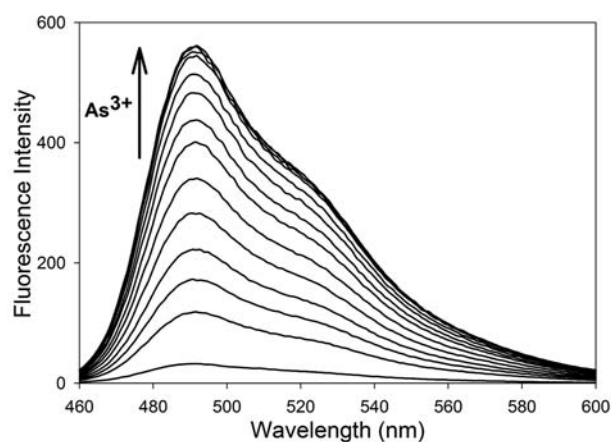


Figure 3. (Top) Fluorescence response of 0.45 μM AF2 in THF at 298 K ($\lambda_{\text{ex}} = 443$ nm). Spectra shown are for $[\text{As}^{3+}]$ (as AsI_3) of 0, 0.26, 0.53, 0.79, 1.05, 1.31, 1.56, 1.84, 2.10, 2.36, 2.62, 2.88, 3.15, 3.41, 3.93, 4.45, 4.97, 5.49, and 6.78 nM. Each reading was obtained 30 min after the addition of As^{3+} . The arrow shows the direction of change. (Bottom) Fluorescence responses of AF2 to various ions (avg. of three trials) under identical conditions. Bars represent the final integrated fluorescence response (F) over the initial integrated emission (F_0). White bars represent the addition of the appropriate ion (4.5 μM) to a 0.45 mM solution of AF2. Gray bars represent the addition of 4.5 μM As^{3+} to the AF2 + ion solutions.

fluorescence enhancement reported for AF1 ($\Phi_f(\text{As}) = 0.101$; $\lambda_{\text{em}} = 496$ nm).¹⁷ Furthermore, the turn-ON response of AF2 is sensitive to low $[\text{As}^{3+}]$, and a detection limit of 0.14 ± 0.03 ppb (0.31 nM) was measured by calculating the concentration that afforded a signal-to-background ratio ≥ 3 .²⁵ This limit is comparable to AF1, which has a detection limit of 0.24 ppb. The detection limits for both AF1 and AF2 are well below the EPA established MCL of 10 ppb for As in drinking water. The AF-to-C6 conversion and corresponding fluorescence emission is also highly selective for As^{3+} , and the fluorescence response of AF1 and AF2 with other metals is minimal (Figure 3, bottom). Indeed, addition of a 10-fold excess of a variety of metal ions to a 0.45 μM THF solution of AF2 resulted in virtually no turn-ON fluorescence; however, addition of As^{3+} to these solutions resulted in immediate fluorescence enhancement (Figure 3, bottom). The fluorescence response in the presence of alkali/alkali-earth metals, first-row transition metals, and other toxic ions like Pb^{2+} and Hg^{2+} was minimal compared to the approximate 20-fold turn-ON after adding As^{3+} . Potential interferences are noted in the presence of Cu^{2+} and to a lesser

extent Co^{2+} , the latter of which is unlikely to be present in significant amounts in water (≤ 2 ppb in drinking water; ~ 100 ppb in contaminated water).²⁹

The spectrophotometric responses of the AFs to ppb levels of As^{3+} establish that AFs can be employed as precursors to the C6 dyes with applications in environmental detection of As compounds or in biological studies with a high As-selectivity/sensitivity. While the AFs clearly react with As^{3+} in organic solvents such as THF, our aim was to use these constructs for monitoring environmental As^{3+} in the form of arsenite. Since the AFs are not entirely water-soluble, we examined the arsenite reaction of AF1 in a THF/ H_2O mixture. AF1 was selected due to its enhanced air stability (*vide supra*), and the reaction of AF1 with As^{3+} salts (AsI_3 or NaAsO_2) was monitored by UV-vis and fluorescence spectroscopies in a THF/CHES (1:1, pH 9) mixed solvent system at 298 K. In each case, the UV-vis maximum at ~ 390 nm disappeared with the formation of a new peak at ~ 470 nm, which is nearly identical to the UV-vis of C6- CF_3 under the same conditions (Figures 4 and S4, Supporting Information). An isosbestic point at 420 nm is also observed in the mixed medium indicating a clean transformation. It should also be noted that the rate of transformation from AF1 to C6- CF_3 is slower in the aqueous THF mixture compared to neat THF with the transformation

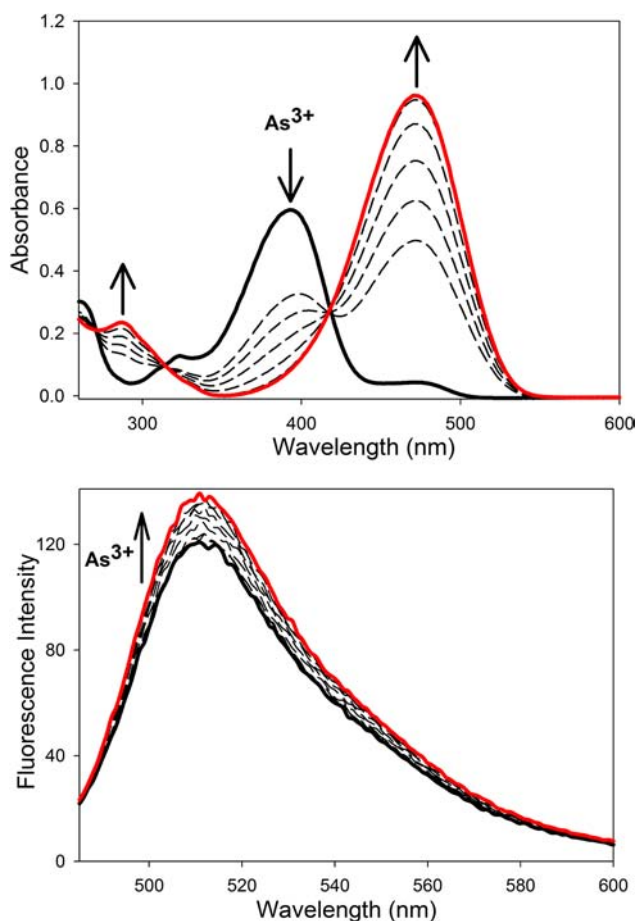


Figure 4. (Top) UV-vis spectral monitoring of the reaction of AF1 ($19.0 \mu\text{M}$) and AsI_3 . Scan intervals are 30 min for 3 h total. (Bottom) Fluorescence response of $0.98 \mu\text{M}$ AF1 to AsI_3 . Scan intervals are 30 min for 4 h total time. All spectra recorded in THF/CHES (1:1, pH 9) at 298 K. Initial trace (bold black) and final trace (bold red). Arrows display direction of change upon addition of As^{3+} .

being complete in 2.5 h versus 0.5 h in THF when using AsI_3 (see Figures 4, top, and S4, Supporting Information, in comparison to Figure S1, Supporting Information). In contrast, the AF1 and NaAsO_2 reaction appeared to stop at a 5 h reaction time with $\sim 50\%$ of the AF1 converted to C6- CF_3 based on extinction coefficient. The fluorescence λ_{em} of C6- CF_3 in THF/CHES (1:1, pH 9) is centered at 509 nm (λ_{ex} : 473 nm), a ~ 15 nm red-shift compared to λ_{em} of 496 nm in THF although the intensity is low. Addition of AsI_3 or NaAsO_2 to AF1 in the aqueous mixture afforded a modest but inconsistent change in the fluorescence intensity (~ 1.2 – 3 -fold increase, Figures 4, bottom, and S5, Supporting Information). While this result is not ideal for fluorescence sensing, the AFs do appear to react and report As^{3+} as demonstrated by the colorimetric response, which is consistent with C6- CF_3 formation. Additionally, the colorimetric response is sensitive to arsenite. The decreased yield of C6- CF_3 (with NaAsO_2) coupled with the induced quenching from the polar medium contributes to the poor fluorometric response of the AFs in an aqueous solvent. This quenched fluorescence has been noted for fluorophores that operate via an internal charge-transfer (ICT) mechanism such as C6 and its derivatives due to the polarity of the excited state molecule.³⁰

The interaction of As^{3+} with the AFs largely resulted in the formation of C6 derivatives, which are responsible for the photoemissive response. To gain further insight into the mechanism of the As^{3+} -promoted redox rearrangement of the benzothiazoline group in AFs, we performed and analyzed products formed from bulk reaction of AFs and As^{3+} . The bulk reaction and analysis of AF1 with As^{3+} has been previously reported by our group.¹⁷ The ^1H NMR spectrum of the bulk indicated that a mixture of C6- CF_3 and a Schiff-base compound was formed.¹⁷ At the time, it was unclear if the Schiff-base was As-bound or not. To clarify this issue in the present account, we synthesized the Schiff-base disulfide analog (SB1) of the AFs for comparison purposes (*vide supra*). Comparison of the ^1H NMR spectrum of SB1 with the AF1 and As^{3+} reaction mixture clearly revealed its formation. Thus, reaction of As^{3+} and AF1 resulted in an equal distribution (based on proton integration) of C6- CF_3 (fluorescent material) and SB1 (Figure 5), which amounts to a 0.5 mol-equiv to 0.25 mol-equiv formation of C6- CF_3 and SB1, respectively, with respect to AF1. The product of the bulk reaction of AF2 and As^{3+} reveals a somewhat similar product distribution in terms of C6 and SB2; however, more SB2 is observed in this case (see Supporting Information, Figures S10 and S11).

The NMR experiments revealed that other nonfluorescent products form in the reaction of AFs with As^{3+} . An As-ligated species is presumably traversed in this process; however, ^1H NMR is consistent with the free and unbound Schiff-base disulfides SB1 and SB2. The oxidation of AFs to form the oxidized analogs (C6 or SB) involve the loss of two electrons and one proton, which would imply the formation of an As^+ center in the sensing mechanism (*vide infra*). To test this hypothesis, bulk reactions as usual were followed by the addition of stoichiometric diphenylphosphinoethane (dppe), a chelating diphosphine ligand known to form a complex with As^+ .^{23,31} Under identical sensing conditions (5 mol-equiv Et_3N , THF, RT), the AFs were reacted with As^{3+} for 30 min after which dppe was added and the product obtained was characterized by ESI-MS and ^{31}P NMR (Figure 6). The most intense peak in the positive mode ESI-MS at m/z 473.0 was in-line with the As^+ complex, $[\text{As}(\text{dppe})]^+$ (Figures 6 and S13,

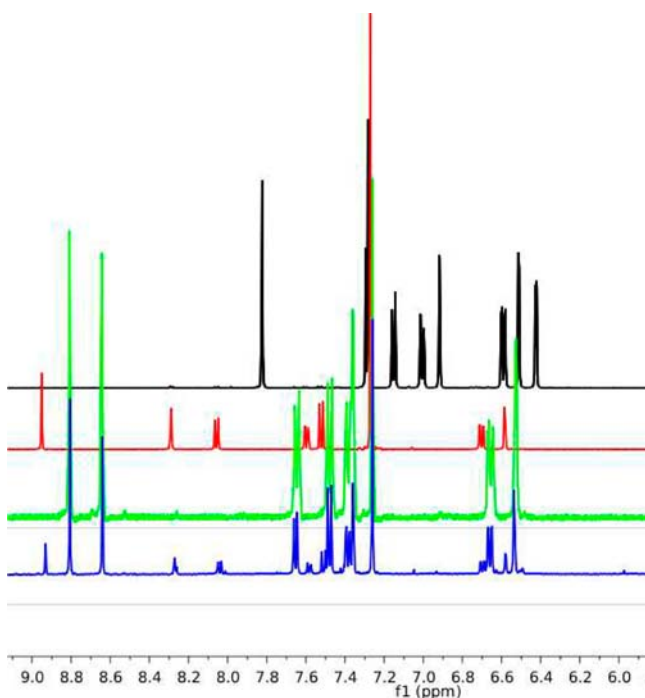


Figure 5. ^1H NMR spectra of the reaction of AF1 + AsI_3 (blue), AF1 (black), independently synthesized C6- CF_3 (red), independently synthesized SB1-disulfide (green) in CDCl_3 . See Figure S12, Supporting Information, for full spectrum.

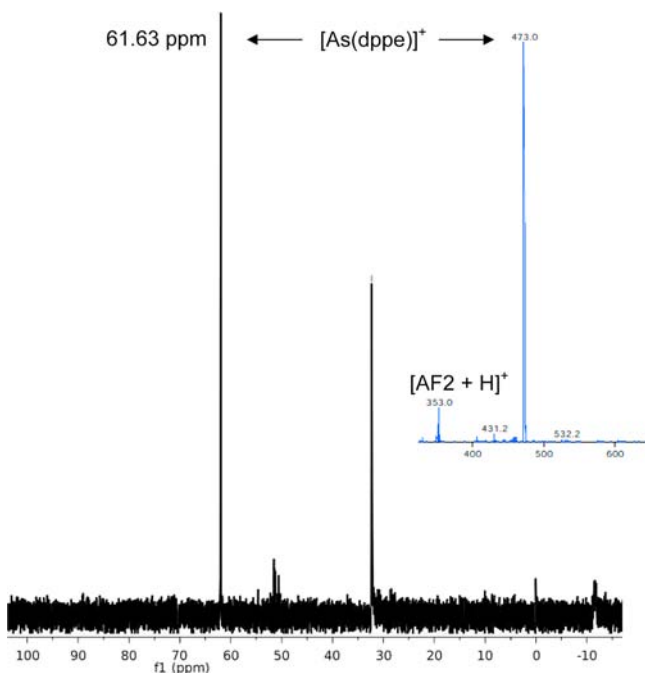


Figure 6. ^{31}P NMR spectrum of the reaction of AF2 and AsI_3 under sensing conditions after the addition of dppe in CD_2Cl_2 . (Inset) Positive mode ESI mass spectrum of the same reaction.

Supporting Information). Other peaks present in the ESI-MS are as expected, i.e., m/z 353.0 (AF2) and m/z 703.2 (SB2). The ^{31}P NMR further confirmed the formation of $[\text{As}(\text{dppe})]^+$ with an intense ^{31}P resonance at 61.63 ppm (CD_2Cl_2 vs external H_3PO_4) (Figure 6).^{23,31} Other less intense peaks are present in the ^{31}P NMR, which have been observed in independent preparations of $[\text{As}(\text{dppe})]^+$ and are attributed to

phosphine oxide formation.²³ Collectively, these results indicated that a loosely bound or free As species is present in the reaction mixture and is easily intercepted with the dppe chelate suggesting an As^+ oxidation state.

Cyclic voltammetry (CV) measurements of the As^{3+} and AF reaction products were also carried out under sensing conditions to further support the NMR results and perhaps imply the formation of an As-ligated complex. Two quasi-reversible waves ($E_{1/2}$: 0.97 V, ΔE_p : 0.11 V; $E_{1/2}$: 0.67 V, ΔE_p : 0.18 V vs Fc/Fc^+) and one irreversible wave (E_{ox} : 0.51 V vs Fc/Fc^+) are observed in the CV of the reaction mixture (Figure 7).

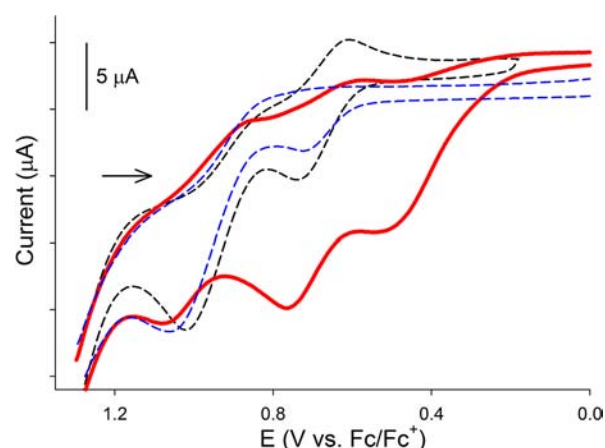


Figure 7. Cyclic voltammograms of THF solutions of the AF1 and As^{3+} reaction mixture (red-solid trace), authentic C6- CF_3 (black-dashed trace), and authentic SB1 (blue-dashed trace) (0.1 M $t\text{Bu}_4\text{NPF}_6$ supporting electrolyte, glassy carbon working electrode, Pt-wire counter electrode, 100 mV/s scan speed, RT).

These resemble events from independently synthesized C6- CF_3 and SB1 (see Figure 7) with the exception of the irreversible oxidation wave at 0.51 V, which we tentatively assign as an As-ligated complex.

DISCUSSION

The synthesis of the As-sensing benzothiazoline compounds, AF1 and AF2, is straightforward and readily achieved in high yields by coupling aldehyde I with a variety of aromatic aminobenzene thiolates. This route is also amenable to modifications on the aminothiols and even with aliphatic aminothiols. For example, reaction of cysteine or homocysteine with I has been exploited for the fluorescence detection of these biological thiols via an ON–OFF photoresponse due to formation of the highly quenched thiazolidine and thiazinane, respectively.^{18b} In contrast to this quenched detection strategy, we have taken advantage of the highly emissive benzothiazoles C6- CF_3 and C6 in an OFF–ON fluorescence response. As such, the AF molecules reported here behave as As-specific sensors in organic (THF) and mixed organic/aqueous media (THF/pH 9 CHES), which are relatively stable as solids and in solution. No spontaneous oxidation from benzothiazoline-to-benzothiazole was observed when mM solutions of AF1 are exposed to aerobic laboratory conditions over 24 h indicating aerobic stability and the low probability of false positive readings due to the presence of adventitious oxygen. This aerobic stability is unique as air-oxidation of benzothiazolines is common.^{19,27c} Indeed, AF2 ($\sim 10\%$ by ^1H NMR in CDCl_3 at RT) oxidized to C6 under the same aerobic lab environment

(24 h), and thus, strict anaerobic conditions are required when using this molecule for As-sensing. AF1 likely derives its oxidative stability from the electron-withdrawing CF₃ group that is *para* to the sulfur, which has a relatively high Hammett constant among common types of aromatic functionalities (σ_p : 0.54).³² The presence of this functional group averts the amount of positive charge that can buildup on the sp³ hybridized carbon (bonded to S and N) in the five-member benzothiazoline ring, which prevents facile loss of the hydride to form the C=N bond of the benzothiazole C6 compounds. Although not undertaken in this study, a thorough Hammett analysis would establish this point more firmly and would assist in the criteria for future use of such molecules for sensing purposes. In fact, the oxygen instability of AF2 has already been utilized to sense the activity of certain redox enzymes. For example, the Hg²⁺ complex of the Schiff-base thiolate form of AF2 has been synthesized and exhibits low fluorescence.¹⁹ However, thiols such as GSH remove the Hg²⁺ cation in the form of an [Hg(SG)₂] complex, which then forms AF2 that slowly oxidizes to generate the fluorescent C6 molecule. This particular reactivity has been used to detect the activity of the enzyme, glutathione reductase, which reduces GSSG to GSH to assist in redox homeostasis in the cell.¹⁹ Thus, the AF compounds in different forms can be used for a variety of sensing purposes.

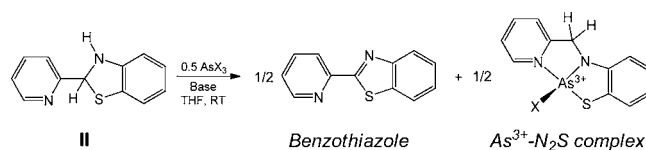
The photophysical properties of the AFs are dominated by the intense charge-transfer transitions from the coumarin chromophore. A significant red-shift of λ_{max} resulted from the extension of the π -system when going from AF-to-C6 and effectively lowers the n - π^* energy gap. X-ray crystallography has established the extension of the π -system in these compounds as the coumarin and benzothiazoline planes are nearly orthogonal in AF1¹⁷ whereas C6 is entirely planar.³³ This UV-vis change also serves as a suitable spectroscopic benchmark for monitoring this transformation when As³⁺ ions are added to THF solutions of AF1 or AF2. Both the UV-vis and fluorescence spectra of the AF and As³⁺ reactions clearly indicated the formation of the C6 derivatives over a 30 min time frame in THF. The emission properties of coumarin-based fluorophores are based on an ICT from the Et₂N-group to the coumarin ring.^{18b,28} However, the quantum yields (Φ_f) of AF1 and AF2 are 0.004 and 0.007, respectively; i.e., these compounds are nonfluorescent. The low fluorescence of the AFs is due to a photoinduced-electron transfer (PET) between the thiazoline nitrogen lone-pair and the coumarin fluorophore, which lead to effective quenching of fluorescence as established in previous studies.^{18b} The >20-fold emission increase in the presence of As³⁺ is due to the formation of the conjugated benzothiazole analog and restoration of the ICT in the planar and rigid C6 derivatives. This reaction appears to be selective for As³⁺ as common metal ions do not elicit any fluorescence response except for Cu²⁺. Silane derivatives such as dimethyldichlorosilane and trimethylchlorosilane have also been reported to promote the oxidation of benzothiazoline rings to the planar benzothiazoles although detailed mechanistic studies and product analyses are lacking.³⁴ Other common metal ions and metalloids do not appear to induce oxidation of the AFs. Collectively, the AF turn-ON is sensitive to low [As³⁺] and selective for As³⁺ over competing metal ions or metalloids that are found in environmental samples with detection limits in the sub ppb range in THF (0.24 and 0.14 ppb for AF1 and AF2, respectively).

The AFs also behave similarly in mixed aqueous conditions with formation of C6 and C6-CF₃ when using As³⁺ sources such as NaAsO₂, a common environmental species. The rate of formation was slower in the aqueous mixture, but the result was the same, i.e., formation of the benzothiazole compounds C6 or C6-CF₃ as monitored by UV-vis spectroscopy. While these aqueous conditions resulted in formation of C6 and would presumably allow for detection of aqueous As³⁺, the fluorescence response was minimal (~2-fold turn-ON). The quenched fluorescence of C6 is attributed to the increased polarity (with respect to THF) of the medium as coumarin-based fluorophores like C6 and C6-CF₃ have been reported for similar molecules where an ICT emission mechanism is evoked.³⁰ Nagano reported a Φ_f of 0.08 for C6 in pH 7.4 sodium phosphate buffer.³⁵ Additionally, C6 formation is significantly slower in THF/CHES (1:1, pH 9), which is evident in the UV-vis monitor of the reaction (see Figure 4, top). However, complete conversion to C6 is observed when As³⁺ salts such as AsI₃ are used. NaAsO₂, a probable species in environmental samples, only partially converts AF1-to-C6 over a similar time frame. While arsenite has proven to have relatively high affinities toward thiols like cysteine and GSH,¹¹ cleavage of the As-O bond in the present study appears difficult to overcome.

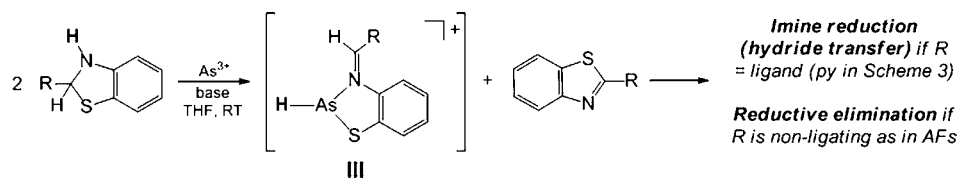
Insight into the mechanism of the sensing process has been provided by spectroscopic analysis of the bulk reaction mixture of the AFs and As³⁺ in THF. For example, ¹H NMR spectroscopy of the bulk has provided evidence for the formation of C6 and C6-CF₃ and the Schiff-base disulfide compounds, SB1 and SB2 in the reaction of As³⁺ with AF1 and AF2, respectively. Both SB compounds formed in the bulk analysis appear to be consistent with an As-nonligated compound. It is interesting to note that a similarly characterized Schiff-base thiolate compound analogous to SB2 with an N,S-coordinated Hg²⁺ center has been characterized by ¹H NMR and the spectrum appears comparable to free SB2.¹⁹ Thusly, the chemical shift values of SB1 and an As-ligated SB1 may be similar; however, one would expect some small difference if arsenic was bound. Further evidence in support of the NMR studies was provided by electrochemistry, which demonstrated the presence of C6, SB, and As compounds in the CV. On the basis of these studies and the established reactivity of benzothiazolines with Cu centers,³⁶ we believe this proposal to be likely.

We previously reported the reaction chemistry of As³⁺ with 2-pyridylbenzothiazoline (II) that resulted in the formation of the 2-pyridylbenzothiazole and the As³⁺-ligated and reduced amide form of II (see Scheme 3). Since the reaction of compounds such as II with transition metals generally furnish Schiff-base thiolate coordination complexes,^{27a} the As³⁺ disproportionation reaction was surprising. In light of this

Scheme 3. Overall Reaction of 2-Pyridylbenzothiazoline (II) with As³⁺



^aX = Cl⁻ or I⁻. Adapted from reference 26. Copyright 2010 American Chemical Society.

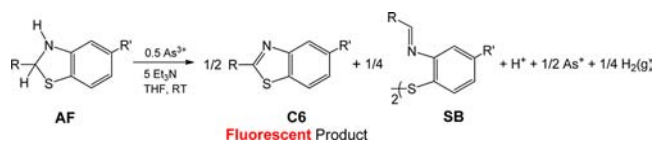
Scheme 4. Proposed Reaction Path for As^{3+} with Benzothiazoline Compounds^a

^aBracketed molecules represent putative transient species.

finding, our original idea for this work was to utilize the defined chemical reaction between benzothiazolines (AFs) and As^{3+} to form fluorescent benzothiazoles (C6) and the As^{3+} ligated amide as a means of detecting this toxic metalloid. While this exact reaction was not the case for the AFs, a comparison between these two reactions has shed light into possible mechanistic issues.

The proposed first steps of the reaction path for the As reaction with **II** or the AFs are the same and lead to one common intermediate, namely, an As^{3+} -hydride complex. It is the fate of the proposed hydride intermediate that differentiates the end-products of these two reactions (Scheme 4). For As^{3+} and **II**, we propose that one benzothiazoline rearranges into the benzothiazole via attack of the thiolate on the Schiff-base nitrogen when bound to As^{3+} , eventual hydride loss, C=N formation resulting in benzothiazole, and generation of the putative As^{3+} -hydride intermediate (**III**). Similar rearrangement chemistry has been noted for the copper-mediated formation of benzothiazoles from an imine disulfide precursor utilizing the $\text{Cu}^{3+/+}$ redox couple.³⁶ In this case, however, a coordinated Cu^+ -thiol intermediate is invoked following formation and release of the benzothiazole. Nevertheless, precedence for this type of rearrangement chemistry of benzothiazolines exists when coordinated to Cu ,³⁶ Re ,³⁷ and Au .³⁸ While precedence for As-hydride complexes with the exception of arsine is scarce, hydride-ligated intermediates with phosphorus have recently appeared.³⁹ Additionally, benzothiazolines are well-established as hydride sources in the Brønsted acid catalyzed reduction of imines and other functionalities to chiral amines.⁴⁰ The fate of the hydride intermediate in the case of **II** is at the azomethine carbon, i.e., where hydride transfer takes place to result in an sp^3 -hybridized carbon and generation of the As^{3+} - N_2S complex with a deprotonated amide-N-ligand (Schemes 3 and 4).⁴¹ All end-products of this reaction have been extensively characterized by crystallography, spectroscopy, and microanalysis.²⁶ After formation of the As^{3+} -hydride intermediate **III** in the AFs, one of two reactions may occur: (i) hydride transfer and formation of the reduced amide as in the case with **II** or (ii) reductive elimination of the intermediate in the form of $\text{H}_2(\text{g})$ and the coordinated thiolate to form the disulfide and As^+ . All evidence (UV-vis, fluorescence, ^1H NMR, dppe reactivity) obtained supports the latter pathway. We propose the controlling factor of hydride transfer versus reductive elimination is likely in coordination of the py-N ligand of **II** providing an accessible and electrophilic azomethine C from the $\text{R}-\text{C}=\text{N}-$ group that is in close proximity. This group is freely rotating in the AFs that do not provide an extra ligating atom. Of course, other factors come into consideration such as the redox potential of the azomethine-C in **II** and the AFs, although one would suspect the potential difference is not too significant, which would favor our proximity argument. Nonetheless, this proposal explains the formation of the fluorescent benzothiazole compounds (C6,

C6- CF_3), the presence of As^+ (as deduced by ESI-MS and ^{31}P NMR when dppe is added), and the Schiff-base disulfides SB1 and SB2 (NMR, ESI-MS, UV-vis). The overall reaction for the AFs is depicted in Scheme 5.⁴¹

Scheme 5. Overall Reaction of AFs with As^{3+} ^a

^aR = diethylaminocoumarin (see Scheme 2); R' = CF_3 (AF1 and C6- CF_3), H (AF2 and C6).

CONCLUSIONS

In summary, we have synthesized and spectroscopically characterized a series of coumarin-appended benzothiazolines, namely, AF1 and AF2, as chemodosimeters for the fluorescence detection of As^{3+} cations. The corresponding Schiff-base disulfides of the AFs (SB1 and SB2) and the benzothiazoles (C6- CF_3 and C6) have also been independently synthesized and spectroscopically characterized as these are likely products in the As^{3+} reaction with the AFs. Indeed, the reaction of the AFs with As^{3+} salts (AsCl_3 , AsI_3) in THF elicited a 20–25-fold increase in fluorescence intensity at $\lambda_{\text{em}} \sim 500$ nm, which is consistent with the formation of the C6 derivatives in this reaction. This result established their ability to detect this toxic metalloid. Furthermore, the AFs are sensitive and relatively selective to low and environmentally relevant concentrations of As^{3+} with detection limits in the sub-ppb range. While the AFs behave excellently in THF, their reactions with As^{3+} (from either simple salts such as AsI_3 or sodium arsenite) in an aqueous medium do not result in a dramatic fluorescence increase, which is likely due to the quenched nature of C6 and its derivatives in high polarity solvents. In light of the nonideal behavior in water mixtures, the AFs do show potential promise for colorimetric detection of As^{3+} as the same products appear to form in THF and water mixtures based on UV-vis spectroscopy. Bulk analysis of the As^{3+} -AF reactions in THF revealed that the reaction path of As^{3+} with benzothiazolines such as the AFs is to form the corresponding benzothiazole and Schiff-base disulfide through a putative As^{3+} -hydride-ligand intermediate. We propose that this intermediate is a common species that is traversed in the reaction of As^{3+} with any benzothiazoline and the ultimate fate depends on the nature of the benzothiazoline. This new reaction may reveal ways to harness the $\text{H}_2(\text{g})$ that is evolved or for the catalytic reduction of imines using benzothiazolines as hydride donors in the presence of As^{3+} . Thus, the AFs have revealed new ways to detect As via a defined As-promoted reaction as well as potential benefits of controlling this chemistry for catalytic

purposes. A fundamental understanding of the reaction chemistry of As^{3+} for field-applicable measurements is ongoing in our lab.

■ ASSOCIATED CONTENT

📄 Supporting Information

UV-vis and fluorescence spectra of AF1, C6-CF₃, and SB1 (in THF and THF/CHES 1:1, pH 9), UV-vis and fluorescence monitor of AF1 and AsI₃ or NaAsO₂, ¹H/¹³C NMR of SB1 and SB2, bulk ¹H NMR of the AF2 + AsI₃ reaction, and ESI-MS of the AF2 + AsI₃ reaction after the addition of dppe. This material is available free of charge via the Internet at <http://pubs.acs.org>.

■ AUTHOR INFORMATION

Corresponding Author

*E-mail: tharrop@uga.edu.

Notes

The authors declare no competing financial interest.

■ ACKNOWLEDGMENTS

T.C.H. acknowledges support from the National Science Foundation (NSF), the University of Georgia Research Foundation (UGARF), and the UGA Department of Chemistry for startup funds.

■ REFERENCES

- (1) (a) Wolfe-Simon, F.; Blum, J. S.; Kulp, T. R.; Gordon, G. W.; Hoefft, S. E.; Pett-Ridge, J.; Stolz, J. F.; Webb, S. M.; Weber, P. K.; Davies, P. C. W.; Anbar, A. D.; Oremland, R. S. *Science* **2011**, *332*, 1163. (b) Csabai, I.; Szathmáry, E. *Science* **2011**, *332*, 1149. (c) Benner, S. A. *Science* **2011**, *332*, 1149. (d) Schoepp-Cothenet, B.; Nitschke, W.; Barge, L. M.; Ponce, A.; Russell, M. J.; Tsapin, A. I. *Science* **2011**, *332*, 1149. (e) Borhani, D. W. *Science* **2011**, *332*, 1149. (f) Cotner, J. B.; Hall, E. K. *Science* **2011**, *332*, 1149. (g) Oehler, S. *Science* **2011**, *332*, 1149. (h) Redfield, R. J. *Science* **2011**, *332*, 1149. (i) Foster, P. L. *Science* **2011**, *332*, 1149. (j) Wolfe-Simon, F.; Blum, J. S.; Kulp, T. R.; Gordon, G. W.; Hoefft, S. E.; Pett-Ridge, J.; Stolz, J. F.; Webb, S. M.; Weber, P. K.; Davies, P. C. W.; Anbar, A. D.; Oremland, R. S. *Science* **2011**, *332*, 1149. (k) Erb, T. J.; Kiefer, P.; Hattendorf, B.; Günther, D.; Vorholt, J. A. *Science* **2012**, *337*, 467. (l) Reaves, M. L.; Sinha, S.; Rabinowitz, J. D.; Kruglyak, L.; Redfield, R. J. *Science* **2012**, *337*, 470.
- (2) (a) Arsenic in your juice. How much is too much? Federal limits don't exist. *Consumer Reports Magazine*; Consumers Union of U.S., Inc.: Yonkers, NY, 2012; <http://www.consumerreports.org/cro/magazine/2012/01/arsenic-in-your-juice/index.htm>; (b) Jackson, B. P.; Taylor, V. F.; Karagas, M. R.; Punshon, T.; Cottingham, K. L. *Environ. Health Perspect.* **2012**, *120*, 623.
- (3) (a) Ferguson, J. F.; Gavis, J. A. *Review of the Arsenic Cycle in Natural Waters*; Pergamon Press: London, 1972; (b) Saha, J. C.; Dikshit, A. K.; Bandyopadhyay, M.; Saha, K. C. *Crit. Rev. Environ. Sci. Technol.* **1999**, *29*, 281. (c) Christen, K. *Environ. Sci. Technol. A Pages* **2001**, *35*, 184A. (d) Garbarino, J. R.; Bednar, A. J.; Rutherford, D. W.; Beyer, R. S.; Wershaw, R. L. *Environ. Sci. Technol.* **2003**, *37*, 1509. (e) Rutherford, D. W.; Bednar, A. J.; Garbarino, J. R.; Needham, R.; Staver, K. W.; Wershaw, R. L. *Environ. Sci. Technol.* **2003**, *37*, 1515. (f) Bednar, A. J.; Garbarino, J. R.; Ferrer, I.; Rutherford, D. W.; Wershaw, R. L.; Ranville, J. F.; Wildeman, T. R. *Sci. Total Environ.* **2003**, *302*, 237. (g) Bissen, M.; Frimmel, F. H. *Acta Hydrochim. Hydrobiol.* **2003**, *31*, 9. (h) Bednar, A. J.; Garbarino, J. R.; Ranville, J. F.; Wildeman, T. R. *J. Agric. Food Chem.* **2002**, *50*, 7340.
- (4) (a) Stone, R. *Science* **2008**, *321*, 184. (b) Okkenhaug, G.; Zhu, Y.-G.; He, J.; Li, X.; Luo, L.; Mulder, J. *Environ. Sci. Technol.* **2012**, *46*, 3155. (c) Li, R. Y.; Stroud, J. L.; Ma, J. F.; McGrath, S. P.; Zhao, F. J. *Environ. Sci. Technol.* **2009**, *43*, 3778. (d) Williams, P. N.; Islam, S.; Islam, R.; Jahiruddin, M.; Adomako, E.; Soliaman, A. R. M.; Rahman,

G. K. M. M.; Lu, Y.; Deacon, C.; Zhu, Y.-G.; Meharg, A. A. *Environ. Sci. Technol.* **2009**, *43*, 8430.

(5) (a) Mandal, B. K.; Suzuki, K. T. *Talanta* **2002**, *58*, 201. (b) Kozul, C. D.; Ely, K. H.; Enelow, R. I.; Hamilton, J. W. *Environ. Health Perspect.* **2009**, *117*, 1441. (c) Kozul, C. D.; Hampton, T. H.; Davey, J. C.; Gosse, J. A.; Nomikos, A. P.; Eisenhauer, P. L.; Weiss, D. J.; Thorpe, J. E.; Ihnat, M. A.; Hamilton, J. W. *Environ. Health Perspect.* **2009**, *117*, 1108.

(6) Tokar, E. J.; Diwan, B. A.; Waalkes, M. P. *Environ. Health Perspect.* **2010**, *118*, 108.

(7) International Agency for Research on Cancer. *IARC Monographs on the Evaluation of Carcinogenic Risks to Humans: Some Metals and Metallic Compounds*; IARC: Lyon, France, 1998; Vol. 23.

(8) United States Environmental Protection Agency. *Arsenic and Clarifications to Compliance and New Source Monitoring Rule: A Quick Reference Guide*; EPA816-F-01-004; EPA: Washington, D.C., 2001; <http://www.epa.gov/safewater/arsenic/compliance.html>.

(9) Bentley, R.; Chasteen, T. G. *Microbiol. Mol. Biol. Rev.* **2002**, *66*, 250.

(10) (a) Hu, Y.; Su, L.; Snow, E. T. *Mutat. Res./DNA Repair* **1998**, *408*, 203. (b) Styblo, M.; Serves, S. V.; Cullen, W. R.; Thomas, D. J. *Chem. Res. Toxicol.* **1997**, *10*, 27. (c) Lin, S.; Cullen, W. R.; Thomas, D. J. *Chem. Res. Toxicol.* **1999**, *12*, 924.

(11) (a) Rey, N. A.; Howarth, O. W.; Pereira-Maia, E. C. *J. Inorg. Biochem.* **2004**, *98*, 1151. (b) Spuches, A. M.; Kruszyna, H. G.; Rich, A. M.; Wilcox, D. E. *Inorg. Chem.* **2005**, *44*, 2964.

(12) (a) Melamed, D. *Anal. Chim. Acta* **2005**, *532*, 1. (b) Klaue, B.; Blum, J. D. *Anal. Chem.* **1999**, *71*, 1408. (c) Goessler, W.; Kuehnelt, D. *Analytical Methods for the Determination of Arsenic and Arsenic Compounds in the Environment*. In *Environmental Chemistry of Arsenic*; Frakenberger, W. T. J., Ed.; Marcel Dekker Inc.: New York, 2002.

(13) (a) Lim, M. H.; Lippard, S. J. *Acc. Chem. Res.* **2007**, *40*, 41. (b) Miller, E. W.; Chang, C. J. *Curr. Opin. Chem. Biol.* **2007**, *11*, 620. (c) Que, E. L.; Domaille, D. W.; Chang, C. J. *Chem. Rev.* **2008**, *108*, 1517. (d) Domaille, D. W.; Que, E. L.; Chang, C. J. *Nat. Chem. Biol.* **2008**, *4*, 168. (e) Zhang, J. F.; Kim, J. S. *Anal. Sci.* **2009**, *25*, 1271. (f) Nolan, E. M.; Lippard, S. J. *Acc. Chem. Res.* **2009**, *42*, 193. (g) Tomat, E.; Lippard, S. J. *Curr. Opin. Chem. Biol.* **2010**, *14*, 225. (h) Pluth, M. D.; Tomat, E.; Lippard, S. J. *Annu. Rev. Biochem.* **2011**, *80*, 333.

(14) Ramanathan, S.; Shi, W.; Rosen, B. P.; Daunert, S. *Anal. Chem.* **1997**, *69*, 3380.

(15) (a) Liao, V. H.-C.; Ou, K.-L. *Environ. Toxicol. Chem.* **2005**, *24*, 1624. (b) Stocker, J.; Balluch, D.; Gsell, M.; Harms, H.; Feliciano, J.; Daunert, S.; Malik, K. A.; van der Meer, J. R. *Environ. Sci. Technol.* **2003**, *37*, 4743. (c) Tauriainen, S.; Karp, M.; Chang, W.; Virta, M. *Appl. Environ. Microbiol.* **1997**, *63*, 4456. (d) Wells, M.; Gösch, M.; Harms, H.; van der Meer, J. R. *Microchim. Acta* **2005**, *151*, 209. (e) Tani, C.; Inoue, K.; Tani, Y.; Harun-ur-Rashid, M.; Azuma, N.; Ueda, S.; Yoshida, K.; Maeda, I. *J. Biosci. Bioeng.* **2009**, *108*, 414. (f) Parker, K. J.; Kumar, S.; Pearce, D. A.; Sutherland, A. J. *Tetrahedron Lett.* **2005**, *46*, 7043. (g) Prindle, A.; Samayoa, P.; Razinkov, I.; Danino, T.; Tsimring, L. S.; Hasty, J. *Nature* **2012**, *481*, 39.

(16) Siegfried, K.; Endes, C.; Bhuiyan, A. F. M. K.; Kuppardt, A.; Mattusch, J.; van der Meer, J. R.; Chatzinotas, A.; Harms, H. *Environ. Sci. Technol.* **2012**, *46*, 3281.

(17) Ezeh, V. C.; Harrop, T. C. *Inorg. Chem.* **2012**, *51*, 1213.

(18) (a) Wu, J.-S.; Liu, W.-M.; Zhuang, X.-Q.; Wang, F.; Wang, P.-F.; Tao, S.-L.; Zhang, X.-H.; Wu, S.-K.; Lee, S.-T. *Org. Lett.* **2007**, *9*, 33. (b) Kim, T.-K.; Lee, D.-N.; Kim, H.-J. *Tetrahedron Lett.* **2008**, *49*, 4879.

(19) Sheng, R.; Ma, J.; Wang, P.; Liu, W.; Wu, J.; Li, H.; Zhuang, X.; Zhang, H.; Wu, S. *Biosens. Bioelectron.* **2010**, *26*, 949.

(20) Iranpoor, N.; Zeynizadeh, B. *Synthesis* **1999**, 49.

(21) Obtained by treating 2-aminothiophenol with NaOH and 50% hydrogen peroxide.

(22) Fulmer, G. R.; Miller, A. J. M.; Sherden, N. H.; Gottlieb, H. E.; Nudelman, A.; Stoltz, B. M.; Bercaw, J. E.; Goldberg, K. I. *Organometallics* **2010**, *29*, 2176.

(23) Ellis, B. D.; Macdonald, C. L. B. *Inorg. Chem.* **2004**, *43*, 5981.

(24) Quantum yield was determined by absolute measurement made by Nanoco with an integrating sphere setup.

(25) (a) Shiraishi, Y.; Sumiya, S.; Hirai, T. *Chem. Commun.* **2011**, *47*, 4953. (b) Garner, A. L.; Koide, K. *J. Am. Chem. Soc.* **2008**, *130*, 16472.

(26) Ezech, V. C.; Patra, A. K.; Harrop, T. C. *Inorg. Chem.* **2010**, *49*, 2586.

(27) (a) Lindoy, L. F.; Livingstone, S. E. *Inorg. Chim. Acta* **1967**, *1*, 365. (b) Hossain, M.; Chattopadhyay, S. K.; Ghosh, S. *Polyhedron* **1997**, *16*, 143. (c) Lynn, M. A.; Carlson, L. J.; Hwangbo, H.; Tanski, J. M.; Tyler, L. A. *J. Mol. Struct.* **2012**, *1011*, 81.

(28) (a) Suresh, M.; Das, A. *Tetrahedron Lett.* **2009**, *50*, 5808. (b) Ma, W.; Xu, Q.; Du, J.; Song, B.; Peng, X.; Wang, Z.; Li, G.; Wang, X. *Spectrochim. Acta, Part A* **2010**, *76*, 248. (c) Zhou, S.; Jia, J.; Gao, J.; Han, L.; Li, Y.; Sheng, W. *Dyes Pigm.* **2010**, *86*, 123. (d) Hu, M.; Fan, J.; Li, H.; Song, K.; Wang, S.; Cheng, G.; Peng, X. *Org. Biomol. Chem.* **2011**, *9*, 980.

(29) Smith, I. C.; Carson, B. L. *Trace Metals in the Environment*; Ann Arbor Science Publishers, Inc: Ann Arbor, 1981.

(30) Barik, A.; Nath, S.; Pal, H. *J. Chem. Phys.* **2003**, *119*, 10202.

(31) Ellis, B. D.; Carlesimo, M.; Macdonald, C. L. B. *Chem. Commun.* **2003**, 1946.

(32) Hansch, C.; Leo, A.; Taft, R. W. *Chem. Rev.* **1991**, *91*, 165.

(33) Jasinski, J. P.; Paight, E. S. *Acta Crystallogr.* **1995**, *C51*, 531.

(34) Meenakshi, S.; Malhotra, R. *Synth. Commun.* **2011**, *41*, 136.

(35) Komatsu, K.; Urano, Y.; Kojima, H.; Nagano, T. *J. Am. Chem. Soc.* **2007**, *129*, 13447.

(36) (a) Šrogl, J.; Hývl, J.; Révész, Á.; Schröder, D. *Chem. Commun.* **2009**, 3463. (b) Rokob, T. A.; Rulišek, L.; Šrogl, J.; Révész, A.; Zins, E. L.; Schröder, D. *Inorg. Chem.* **2011**, *50*, 9968.

(37) Zhang, C.; Guzei, I. A.; Espenson, J. H. *Inorg. Chem.* **2001**, *40*, 2437.

(38) Koley, A. P.; Nirmala, R.; Prasad, L. S.; Ghosh, S.; Manoharan, P. T. *Inorg. Chem.* **1992**, *31*, 1764.

(39) Dunn, N. L.; Ha, M.; Radosevich, A. T. *J. Am. Chem. Soc.* **2012**, *134*, 11330.

(40) (a) Zhu, C.; Akiyama, T. *Synlett* **2011**, *2011*, 1251. (b) Henseler, A.; Kato, M.; Mori, K.; Akiyama, T. *Angew. Chem., Int. Ed.* **2011**, *50*, 8180. (c) Zhu, C.; Akiyama, T. *Org. Lett.* **2009**, *11*, 4180. (d) Saito, K.; Akiyama, T. *Chem. Commun.* **2012**, *48*, 4573. (e) Zhu, C.; Akiyama, T. *Adv. Synth. Catal.* **2010**, *352*, 1846.

(41) The formation of H₂ in this reaction was not performed due to the experimental challenges associated with the detection of this gas in the small amounts formed in the bulk reaction, which is approximately 11 ppm. While GC methods are available for this type of measurement, the sensitivity of such techniques is not adequate for the bulk reactions performed. For example, typical GC-MS limits for H₂ measurements are in the hundreds of ppm; see Snavely, K.; Subramaniam, B. *J. Chromatogr. Sci.* **1998**, *36*, 191 which reports a detection limit of 200 ppm. Thus, although the formation of H₂ was not experimentally confirmed in this case, isolation and characterization of the other products formed lend some support to the equation depicted in Scheme 4.